

# KINETIC MODELING OF A PHOTOCATALYTIC REACTOR DESIGNED FOR REMOVAL OF GAS-PHASE BENZENE: A STUDY ON LIMITING RESISTANCES USING DESIGN OF EXPERIMENTS

J. KRISHNAN<sup>†</sup> and T. SWAMINATHAN<sup>‡</sup>

<sup>†</sup> Faculty of Chemical Engineering, Universti Teknologi MARA, Shah Alam - 40450, Malaysia.

jagannathan@salam.uitm.edu.my (corresponding author)

<sup>‡</sup> Department of Chemical Engineering, Indian Institute of Technology Madras, Chennai - 600036, India.

tswami@iitm.ac.in

**Abstract**— Experiments were conducted at room temperatures, in an immobilized annular tube reactor, using titanium dioxide as the photocatalyst, to identify the influence of important operational parameters, viz., catalyst load ( $5\text{--}20\text{ g m}^{-2}$ ), benzene concentration ( $0.2\text{--}6\text{ g m}^{-3}$ ) and flow rate ( $0.2\text{--}1\text{ L min}^{-1}$ ) on the removal of benzene. Removal efficiencies for benzene ranged from 7% to 96% depending on the range of levels of these process parameters. A modified Langmuir–Hinshelwood (L–H) kinetic model has been suggested based on the experimental observations. The use of a combined plug–flow type L–H kinetic model yielded a design equation that can be used as the basis for the photoreactor scale-up as well as to find the mass transfer and reaction resistances in the photoreactor. The ratio of reaction rate resistance to the overall resistance was found to play an important role in establishing the predominant resistances between mass transfer and reaction rate occurring in the photoreactor.

**Keywords**— Photocatalysis; gas–phase benzene; Langmuir–Hinshelwood model; immobilized photoreactor.

## I. INTRODUCTION

Both indoor and outdoor air pollution with volatile organic compounds (VOCs) has been a serious environmental problem nowadays due to their carcinogenic nature as well as their tendency to form secondary pollutant, viz., ozone by reacting with  $\text{NO}_x$  in the presence of sunlight at the ground level. Among the different treatment methods developed for the degradation of VOCs, photocatalytic oxidation process can be considered as an innovative and promising technology to completely oxidize high concentrations of VOCs to harmless end products such as  $\text{H}_2\text{O}$  and  $\text{CO}_2$  at ambient temperatures (Wang *et al.*, 2003; Jagannathan *et al.*, 2004).  $\text{TiO}_2$  irradiating with ultraviolet (UV) or near UV light results in the formation of electron–hole pairs on the catalyst surface. These electrons and holes interact with adsorbed species producing highly reactive hydroxyl radicals, which in turn initiate redox reactions to decompose VOCs. As the decreasing wavelength increases the radiant power output of the UV lamps, use of the germicidal lamps (254 nm) for the photodegradation of VOCs was reported to be more efficient (Shen

and Ku, 2002; Pengyi *et al.*, 2003; Jeong *et al.*, 2004 and Jagannathan, Ph.D thesis, 2006). During the last decade, the gas–phase elimination of VOCs has received more attention (Pengyi *et al.*, 2003).

Photoreactors of various configurations have been developed; however, annular fixed-bed reactors with  $\text{TiO}_2$  coated on the surface of reactor wall are the most commonly employed photoreactors for their ease of construction and operation (Ollis and Al-Ekabi, 1993; Alberici and Jardim, 1997; Hennezel *et al.*, 1998). During initial stages of reactor experiments, statistical methodology plays significant role in analyzing the data obtained by studying different process parameters, where there is a likely chance of experimental errors (Montgomery, 1991). However, determining the reaction kinetics is an important aspect of successful design of catalytic reactors. Simple kinetic models help in predicting the expected conversions and also desired size of a reactor. Heterogeneous photochemical reactions, unlike other chemical reactions, are more complex as they involve a variety of mechanisms such as adsorption, surface reaction, desorption etc. It is found from literatures that, kinetic modeling of photoreactors has not been carried out extensively; however, Langmuir–Hinshelwood (L–H) type rate expression has been widely used to describe gas–solid reactions for heterogeneous photocatalysis (Fox and Dulay, 1993; Alberici and Jardim, 1997; Kim and Hong, 2002; Lin *et al.*, 2002). Anew, a wide variety of hydrophilic and hydrophobic VOCs have been tested, that includes, trichloroethylene (Jacoby *et al.*, 1995), 1-butane (Cao *et al.*, 1999), toluene (Bouzaza and Laplanche, 2002), vinyl chloride (Mohseni and David, 2003), hexane (Zhang and Liu, 2004), benzene, toluene, ethylbenzene and xylene (BTEX) in the presence of  $\text{SO}_2$  and  $\text{NO}$  (Ao *et al.*, 2004).

In this study, the use of  $2^k$  factorial design to study the effect of process parameters on the removal of benzene by UV/ $\text{TiO}_2$  process in the annular immobilized photoreactor has been described. Moreover, the effects of catalyst load, inlet benzene concentration and the gas flow rate on the resistance ratio were studied using  $2^k$  factorial design. Later from these results, the main and interaction effects were analyzed for its statistical significance by performing an analysis of variance (ANOVA). The decomposition behavior of gas–phase

benzene in an annular immobilized photoreactor was modeled with a modified Langmuir–Hinshelwood (L–H) type rate equation. Using the kinetic constants evaluated from the experimental data, a resistance ratio was calculated to find whether the photodegradation of benzene was mass transfer controlled or reaction rate controlled.

## II. MATERIALS AND METHODS

### A. Chemicals and analytical methods

The chemicals used in this study, viz., benzene (Ranbaxy chemicals, 99% purity) and TiO<sub>2</sub> (CDH Chemicals, primarily anatase, surface area: 15 m<sup>2</sup> g<sup>-1</sup>), were used without further purification. Gas – phase benzene (2 ml) collected in air – tight syringes from the inlet and outlet sampling ports of the photoreactor were injected in a Gas Chromatograph (Model No: 5765, Nucon Engg. India) fitted with a Chromatopak column (1/8" ID, liquid – 3% Dexil, solid – Ch-W (AW), 80/100 mesh) and a flame ionization detector. Nitrogen was used as the carrier gas at a flow rate of 30 mL min<sup>-1</sup>. The temperatures of the injection port, oven and detection port were 200, 55 and 210 °C respectively. The gas–elution time in the chromatograph was 1.5 min for benzene.

### B. Annular immobilized photoreactor

The schematic of the photoreactor is shown in Fig. 1. This annular type photoreactor (Jagannathan, 2006) consisted of a cylindrical tube, 3.7 cm inner diameter and 43 cm long, was fitted with a cylindrical UV lamp, 2.6 cm diameter and 43.5 cm long by using thread–ended caps. The effective annular volume of the reactor is 234 ml.

### C. Coating procedure

A 10 ml of ultrasonicated TiO<sub>2</sub> slurry was poured inside the reactor, fitted with the end caps and connected to a rotary mechanism. One end was connected to shaft of the motor which was rotated at a speed of 10 rpm and

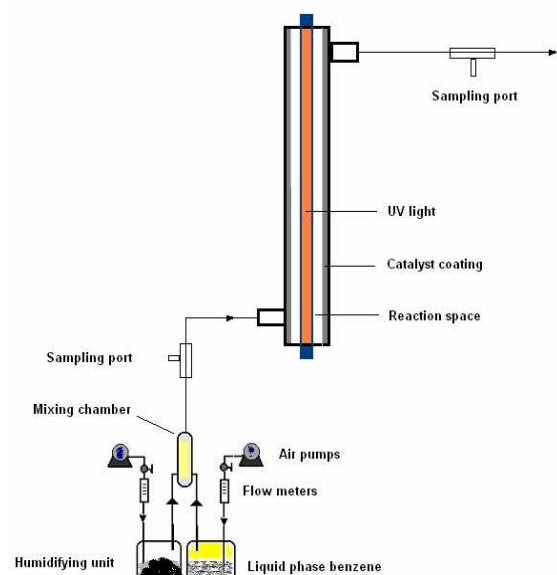


Fig 1. Schematic of the experimental photoreactor setup.

through the other end hot air is blown via an opening provided in the end cap for about 10 minutes. On observing a uniform coating on the inner surface of the tube, reactor was taken out and kept inside the oven for calcination overnight at 200°C.

### D. Experimental

The UV light intensity measured by a hand held digital radiometer was 55 mW cm<sup>-2</sup> (Lutron Electronic Services Co. Ltd., Taiwan). By sparging oil free air through a mini diaphragm air pump into a bottles containing distilled water and benzene resulted in humidified air stream and saturated benzene streams respectively at room temperature which were then mixed in a mixing chamber to produce moist benzene stream. The saturated moist air stream at controlled flow rate was passed through a series of packed columns containing drying agents silica gel and calcium chloride dihydrate to get the required level of relative humidity. The inlet gaseous stream was passed through the reactor without illumination till an equilibrium adsorption is attained. After ensuring steady state, the lamp was turned on and gaseous samples from the inlet and outlet sampling port were analyzed at regular intervals. All the experiments were carried out at ambient temperature (28±2°C) and at a relative humidity of 55%. The performance of the photoreactor was evaluated in terms of removal efficiency (Eq. 1), which is the fraction of benzene removed by the system.

$$\text{Removal Efficiency, \%} = 100 \times (C_{gi} - C_{go}) / C_{gi}, \quad (1)$$

where, C<sub>gi</sub> and C<sub>go</sub> are the inlet and exit benzene concentrations.

### E. Statistical design of experiments

Factorial designs are widely used in situations where several important factors that could have possible interactive effects, are studied on a particular response. The 2–level full factorial design, which is most popular, includes all possible factor combinations at two levels, low and high, for each of the factors. For a process involving 3 factors, viz., catalyst load, gas – phase benzene concentration and flow rate, at 2 levels, a complete replicate of such a design requires 2 × 2 × 2 = 8 experiments (Montgomery, 1991). Analysis of variance (ANOVA) was applied to estimate the effects of main variables and their potential interaction effects on the benzene removal. ANOVA provides valuable information on the following statistical terms, which was later analyzed for their significance.

## III. RESULTS AND DISCUSSION

### A. Effects of process parameters

The effect of three influencing process parameters namely, catalyst load, benzene concentration and flow rate on the removal of benzene was studied in the annular tube – type photoreactor using 2<sup>k</sup> factorial design approach. The level of factors used in this study is given in Table 1. A total of 10 experiments were performed using the combination of these parameters and the removal efficiency in each of the case, after steady state was determined.

Table 1. Level of factors used to determine the removal efficiency of benzene

Parameters	Level of factors		
	-1	0	+1
Catalyst load ( $\text{g m}^{-2}$ )	5	12.5	20
Concentration ( $\text{g m}^{-3}$ )	0.2	3.1	6
Flow rate ( $\text{L min}^{-1}$ )	0.2	0.6	1

Table 2. ANOVA table for Benzene removal.

Source	DF	Seq SS	Adj SS	Adj MS	F	P
Main Effects	3	6692.86	6692.86	2230.95	30000	0.004
2-Way Interactions	3	1026.94	1026.94	342.31	5000	0.01
3-Way Interactions	1	0.14	0.14	0.14	2.13	0.383
Residual Error	1	0.06	0.06	0.06		
Pure Error	1	0.06	0.06	0.06		

Note: **DF**-Degrees of Freedom; **Seq SS**-Sequential Sum of Squares; **Adj SS**-Adjusted Sum of Squares; **Adj MS**-Adjusted Mean of Squares; **F**-Fischer's variance ratio; **P**-Probability value.

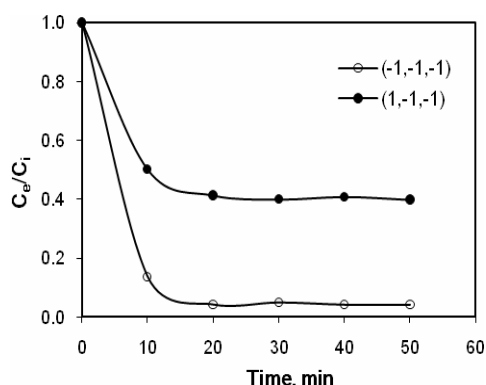


Fig 2. Gas-phase benzene removal profiles versus time for different experimental conditions.

The concentration profiles for the experimental conditions, (-1,-1,-1) and (1,-1,-1) are shown in Fig. 2. It is quite evident that stable removal efficiencies, i.e., steady state conditions were achieved within 10 min of experimental startup. It can be seen that, at constant initial benzene concentration of  $0.2 \text{ g m}^{-3}$  and flow rate of  $0.2 \text{ L min}^{-1}$ , increasing the catalyst load from 5 to  $20 \text{ g m}^{-2}$ , increased the removal of benzene from 60% to 96%. Also, it was observed that, at low levels of catalyst load ( $5 \text{ g m}^{-2}$ ), high benzene concentrations ( $6 \text{ g m}^{-3}$ ) and high gas flow rates ( $1 \text{ L min}^{-1}$ ) reduced the removal of benzene to significantly low values (7%). The elimination capacity for these experimental conditions was found to be in the range of  $1.16$  to  $14.86 \text{ g m}^{-3} \text{ h}^{-1}$ . Since the benzene removal efficiency showed a wide range, from 7% to 96%, it is clearly understandable that some of the process parameters are highly significant in affecting the removal of benzene.

A statistical analysis was later carried out using the software, MINITAB (Version 15.1.3, Minitab Inc., USA) and the results are given in Table 2. In this table, The Fischer variance ratio (F), which is a statistically valid measure of the fitness of the model, can be calculated from the ANOVA table by dividing the mean

square due to model by mean square due to error. The greater the F value from testing, more certain it is that the estimated factors are real. The high F values and low P values (Probability values) show that the main effects ( $F = 30,000$ ,  $P = 0.004$ ) and the 2-way interaction effects ( $F = 5000$ ,  $P = 0.01$ ) are highly significant for the removal efficiency of benzene, than the three way interaction effects. Among the main effects on removal of benzene, benzene concentration ( $T = -286.57$ ,  $P = 0.002$ ) appears to play a major role than catalyst loading rate ( $T = 107.35$ ,  $P = 0.006$ ) and flow rate ( $T = -98.18$ ,  $P = 0.006$ ). Thus, it can be observed that changes in benzene concentration have a greater effect on the removal efficiency of benzene than changes in catalyst load and flow rate. Anew, it was evident that the removal efficiency of benzene increases directly with the increase in the catalyst load and decreases with increase in benzene concentration as well as flow rate. As the catalyst loading rate increases, the available active sites of the catalyst surface increases, thereby more pollutants are adsorbed on the surface of the catalyst leading to the higher removal of pollutants. Similar effect of catalyst on aqueous and gaseous benzene removal was reported by many researchers. Sirisuk *et al.* (1999) reported that ethylene conversion increased with an increase in catalyst loading rate. Lewandowski and Ollis (2003) identified increasing effect of catalyst load on the photocatalytic degradation of benzene.

Higher initial concentration of pollutants (run no. 7) results in decreasing the removal of pollutants by photocatalytic oxidation as the available catalyst surface area of the catalyst becomes insufficient for the excess pollutant molecules. This decreasing trend is consistent with the photocatalytic oxidation results reported for benzene in the literature (Lichtin and Sadeghi, 1998; Wang and Ray, 2000; Wang *et al.*, 2003) Similarly, when the flow rate is lower, the time spent by the pollutants inside the photoreactor is more, yielding higher removal of pollutants and vice versa. Fu *et al.* (1995) observed similar results for the degradation of benzene in an annular photoreactor.

### B. Kinetic modeling and rate-limiting step

The mass transfer rate could be very large and not limiting for a batch reactor (Bouzaza *et al.*, 2006), nevertheless, the rate would be finite and limiting in the case of a continuous reactor. When the tubular reactor is used, it would be interesting to know if the mass transfer rate or the kinetic is the limiting step. Overall mass balances on the gas phase and the solid phase, in a continuous reactor at steady state, give the following equations.

$$\text{Gas phase: } u \frac{\partial C}{\partial Z} + k_m a_v (C - C_s) = 0, \quad (2)$$

$$\text{Solid phase: } k_m a_v (C - C_s) = k \frac{KC_s}{1 + KC_s}, \quad (3)$$

where,  $C$  is the bulk gas-phase concentrations,  $C_s$  represents the concentration near the surface of the photocatalyst. A Langmuir-Hinshelwood mechanism is assumed for the degradation of the benzene. Usually we

can assume that  $KC_s \ll 1$ . Under these conditions the solid phase mass balance can be approximated to:

$$\text{Solid phase: } k_m a_v (C - C_s) = kKC_s, \quad (4)$$

Using Eq. (4) to obtain  $C_s$  and substituting in Eq. (2) and solving the resulting differential equation, the following solution is obtained.

$$\frac{C_s}{C_i} = \exp\left(-k^* \frac{L}{u}\right), \quad (5)$$

where  $k^*$  represents the apparent rate constant ( $\text{min}^{-1}$ ),  $L$ , the length of the reactor,  $C_i$  the inlet concentration and  $u$  the velocity of the gas through the reactor.

The product  $k^*L/u$  is known as the reaction Damkohler number and is dimensionless.  $k^*$  takes into account both the rate of the reaction at the surface of the immobilized catalyst and the mass transfer of the reactant to the surface.  $k^*$  is given by the following equation:

$$\frac{1}{k^*} = \frac{1}{kK} + \frac{1}{k_m a_v}, \quad (6)$$

where  $k$  is the reaction rate constant ( $\text{g m}^{-3} \text{min}^{-1}$ ),  $K$ , the Langmuir adsorption constant ( $\text{m}^3 \text{g}^{-1}$ ),  $k_m$  the mass transfer coefficient from gas to catalyst surface ( $\text{m min}^{-1}$ ) and  $a_v$  the total effective catalyst area per unit volume of the reactor ( $\text{m}^2 \text{m}^{-3}$ ). In Eq. (6), the two terms on the right hand represent respectively the reaction rate and mass transfer resistance.

Equation (5) can be used to obtain the apparent rate constant  $k^*$  from known experimental values of  $C_s/C_i$  at given flow velocity  $u$ . The value of  $C_s$  is assumed to be equal to the outlet concentration  $C_e$ . Assuming that the mass transfer is not the limiting step and that the effect of intermediate product is negligible, then the degradation rate in a plug-flow reactor can be expressed as

$$u \frac{dC}{dZ} = \frac{kKC}{1+KC}, \quad (7)$$

where,  $Z$  represents the axial position in the photoreactor (m). After rearrangement, integration of Eq. (7) for the entire reactor length ( $L$ ) leads to

$$\frac{\ln(C_i/C_e)}{C_i - C_e} = \frac{kKL}{u(C_i - C_e)} - K. \quad (8)$$

If the proposed L-H model is valid, a plot of  $\ln(C_i/C_e)/(C_i - C_e)$  versus  $1/u(C_i - C_e)$  should be linear. The slope should be equal to  $kKL$  and the negative intercept with ordinate axis equal to  $-K$ . Then the comparison between the value of  $kK$  and  $k^*$  obtained respectively from Eq. (8) and (5) will allow the estimation of effect of mass transfer resistance on the photodegradation of the benzene. Equation (8) can be used as a design equation either to predict the outlet concentration after photodegradation or to determine the length of the reactor for a desired removal of benzene. It can also be used as the basis for the photoreactor scale-up. The apparent rate constant  $k^*$  ( $\text{min}^{-1}$ ) takes into account both the rate of the reaction at the surface of the immobilized catalyst and the mass transfer of the reactant to the surface. It can be calculated from known experimental values of  $C_e/C_i$  at given flow velocity  $u$ . When the ratio

$k^*/kK$  approaches 1, the overall mass transfer is equal to the reaction rate constant ( $kK$ ) even if the flow velocity is low. Hence, the mass transfer step will not be the rate limiting step but the photodegradation of the benzene will be reaction rate controlled in the plug-flow reactor.

The L-H plot for benzene removal at a catalyst load of  $12.5 \text{ g/m}^2$  is given in Fig. 3. For fitting the L-H model, half of the data were used to estimate the model parameters while rest the data were used to test the fit of the model. As can be visualized from the figure and from the correlation coefficient value, it is seen that the L-H model fitted the data for photodegradation of benzene in annular immobilized photoreactor very well. Using the constants estimated from the plot and L-H equation, the outlet concentration was predicted and compared with the experimental values. The comparison plot given in Fig. 4 shows that the predictability of the kinetic model is appreciably good because all the data points in the parity plot lie within 4% error.

The ratio of reaction rate resistance to the overall resistance,  $k^*/kK$ , for the benzene removal of given in Table 3. The range of parameters is given in coded values. The Reynolds numbers were calculated for the flow of benzene in the photoreactor and found to be between 2 and 24 which confirmed the laminar flow. Only for a lower benzene concentration of  $0.2 \text{ g m}^{-3}$  and a higher flow rate of  $1 \text{ L min}^{-1}$  and irrespective of the catalyst load, the photodegradation of benzene was found to be reaction rate controlled as the ratio  $k^*/kK$  was greater than 1 even at the laminar flow.

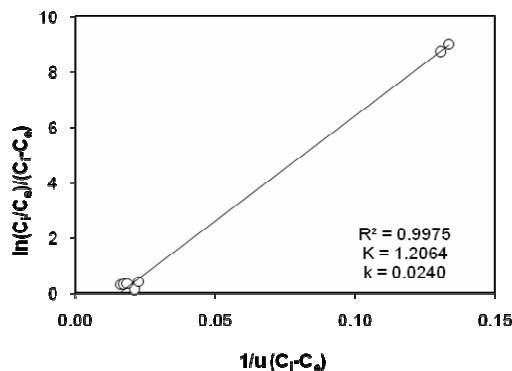


Fig. 3. L-H plot for benzene removal.

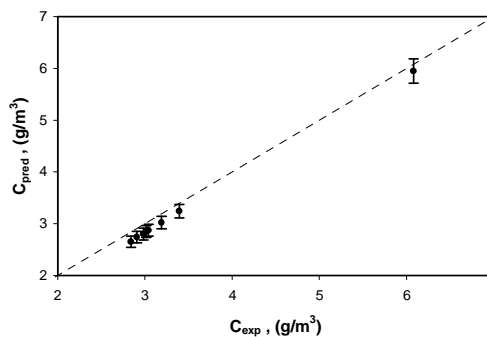


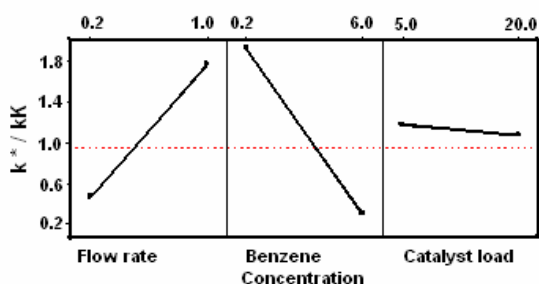
Fig. 4. Comparison between experimental and L-H model predicted outlet concentrations for benzene

Table 3.  $k^*/kK$  for benzene removal at different experimental conditions

Run order	Catalyst load, (g m <sup>-2</sup> )	VOC concentration, (g m <sup>-3</sup> )	Flow rate, (L min <sup>-1</sup> )	$k^*/kK$
1	-1	-1	-1	0.8571
2	-1	-1	1	3.0000
3	-1	1	-1	0.1429
4	-1	1	1	0.7143
5	1	-1	-1	0.8696
6	1	-1	1	3.0435
7	1	1	-1	0.0435
8	1	1	1	0.3478
9	0	0	0	0.1360
10	0	0	0	0.1369

Table 4. ANOVA of  $k^*/kK$  for benzene removal

Source	DF	Seq SS	Adj SS	Adj MS	F	P
Main Effects	3	8.708	8.708	2.9027	10000	0.007
2 - Way Interactions	3	1.521	1.521	0.507	2000	0.018
3 - Way Interactions	1	0.0111	0.0111	0.0111	39	0.102
Residual Error	1	0.0003	0.0003	0.0003		
Pure Error	1	0.0003	0.0003	0.0003		
Total	9	11.7749				

Fig 5. Main effects plot of  $k^*/kK$  for benzene removal.

For all other experimental runs the degradation was mass transfer controlled. Using the semi-empirical Leveque equation (Bird *et al.*, 1984), the mass transfer coefficient ( $k_m$ ) was evaluated. The values obtained were more than 1000 times smaller than  $k^*$ . This confirms that the resistance ( $1/k_m a_v$ ) due to the mass transfer is predominant.

The effect of parameters on the ratio,  $k^*/kK$  can be explained using the factorial plots. By examining the main effects plot as given in Fig. 5, the ratio  $k^*/kK$  was found to increase with increasing flow rate and decrease with increasing benzene concentration.

These phenomena are consistent with the logical fact that lower flow rate leading to mass transfer control and higher flow rate leading to reaction rate control. The effect of catalyst on the ratio  $k^*/kK$  was negligible as the profile lies almost flat. From the analysis of variance given in Table 4, higher  $F$  value and lower  $P$  value indicate that the main and 2-way interaction effects are more significant. Hence all the three parameters namely catalyst load, benzene concentration and flow rate were found to influence the kinetic resistance in the annular photocatalytic reactor.

### C. Practical implications of this study

It is found that the removal rates are quite high if the initial concentration is low. In order to effectively use

the photocatalytic degradation in the industries, where high VOC concentrations are expected, it is recommended that the pollutants can be diluted and then treated using photodegradation. Alternatively, it can also be coupled with other techniques such as biodegradation for the maximum removal of pollutants.

## IV. CONCLUSION

A study on gas-phase benzene removal by photodegradation in an annular tubular photoreactor was performed through a 2<sup>3</sup> factorial design of statistical significance.

It was observed that, changes in benzene concentration (0.2 to 6 g m<sup>-3</sup>) have a greater effect on the removal efficiency of benzene than changes in catalyst load and flow rate. Increase in the catalyst load increased the removal of benzene whereas increase in benzene concentration and flow rate decreased the benzene removal. High removal efficiencies (96%) were attained at a catalyst load of 5 g m<sup>-2</sup>, low initial concentrations of benzene (0.2 g m<sup>-3</sup>) and at low gas flow rates (0.2 L min<sup>-1</sup>).

The kinetic model equation developed based on Langmuir-Hinshelwood (L-H) type kinetics and mass transfer model was found to be useful in predicting the outlet concentration from the photoreactor after treatment, as well as helped to determine the length of the reactor for achieving high removal of VOCs. Furthermore, the developed model was validated by checking the accuracy of prediction of outlet benzene concentrations from the photoreactor. The maximum deviation of the predicted values from the experimental values was found to be 4%.

Another key aspect of this kinetic modeling approach was to determine whether photodegradation was mass transfer controlled or reaction resistance controlled. Only for lower benzene concentration (0.2 gm<sup>-3</sup>) and at a very high gas flow rate of 1 L min<sup>-1</sup>, irrespective of the catalyst load, the photodegradation of benzene was found to be reaction rate controlled. The ratio of  $k^*/kK$  was greater than 1 even at the laminar flow region. For all other experimental runs the degradation was mass transfer controlled.

## ACKNOWLEDGEMENTS

The authors would like to thank and acknowledge the support in terms of research funds received from the Swedish International Development Agency (SIDA) for carrying out this research work. We are grateful to the Universti Teknologi MARA, Shah Alam, Malaysia for computational assistance.

## REFERENCES

- Alberici, R.M. and W.F. Jardim, "Photocatalytic destruction of VOCs in the gas-phase using titanium dioxide," *Applied Catalysis B: Environmental*, **14**, 55-68 (1997).
- Ao, C.H., S.C. Lee, J.Z. Yu and J.H. Xub, "Photodegradation of formaldehyde by photocatalyst TiO<sub>2</sub>: effects on the presences of NO, SO<sub>2</sub> and VOCs," *Applied Catalysis B: Environmental*, **54**, 41-50 (2004).

- Bird R.B., W.E. Stewart and E.N. Lightfoot, *Transport Phenomena*, Wiley, New York (1984).
- Bouzaza, A. and A. Laplanche, "Photocatalytic degradation of toluene in the gas phase: Comparative study of some TiO<sub>2</sub> supports," *Journal of Photochemistry and Photobiology A: Chemistry*, **150**, 207-212 (2002).
- Bouzaza, A., C. Vallet and A. Laplanche, "Photocatalytic degradation of some VOCs in the gas phase using an annular flow reactor Determination of the contribution of mass transfer and chemical reaction steps in the photodegradation process," *Journal of Photochemistry and Photobiology A: Chemistry*, **177**, 212-217 (2006).
- Cao, L., A. Huang, F.J. Spiess and S.L. Suib, "Gas-Phase Oxidation of 1-Butene Using Nanoscale TiO<sub>2</sub> Photocatalysts," *Journal of Catalysis*, **188**, 48-57 (1999).
- Fox, M.A. and M.T. Dulay, "Heterogeneous Photocatalysis," *Chemical Review*, **93**, 341-357 (1993).
- Fu, X., W.A. Zeltner and M.A., "Anderson The gas-phase photocatalytic mineralization of benzene on porous titania-based catalysts," *Applied Catalysis B: Environmental*, **6**, 209-224 (1995).
- Hennezel, O., P. Pichat and D.F. Ollis, "Benzene and toluene gas-phase photocatalytic degradation over H<sub>2</sub>O and HCl pretreated TiO<sub>2</sub>: by-products and mechanisms", *Journal of Photochemistry and Photobiology A: Chemistry* **118**, 197-204 (1998).
- Jacoby, W.A., D.M. Blake, R.D. Noble and C.A. Koval, "Kinetics of the oxidation of Trichloroethylene in air via Heterogenous Photocatalysis," *Journal of Catalysis*, **157**, 87-96 (1995).
- Jagannathan, K., R.A. Damodar and T. Swaminathan, "Heterogeneous photocatalytic oxidation - A versatile technique for removal of hazardous pollutants," *Chemical Engineering World*, **39**, 47-54 (2004).
- Jagannathan, K., "Photocatalytic degradation of volatile organic compounds in an immobilized photoreactor," *Ph.D thesis*, Indian Institute of Technology Madras, India (2006).
- Jeong, J., K. Sekiguchi and K. Sakamoto, "Photochemical and photocatalytic degradation of gaseous toluene using short-wavelength UV irradiation with TiO<sub>2</sub> catalyst: Comparison of three UV sources," *Chemosphere*, **57**, 663-671 (2004).
- Kim, S.B. and S.C. Hong, "Kinetic study for photocatalytic degradation of volatile organic compounds in air using thin film TiO<sub>2</sub> photocatalyst," *Applied Catalysis B: Environmental*, **35**, 305-315 (2002).
- Lewandowski, M. and D.F. Ollis, "A Two-Site kinetic model simulating apparent deactivation during photocatalytic oxidation of aromatics on titanium dioxide," *Applied Catalysis B: Environmental*, **43**, 309-327 (2003).
- Lichtin, N.N. and M. Sadeghi, "Oxidative photocatalytic degradation of benzene vapor over TiO<sub>2</sub>," *Journal of Photochemistry and Photobiology A: Chemistry*, **113**, 81-88 (1998).
- Lin, H.F., R. Ravikrishna and K.T. Valsaraj, "Reusable adsorbents for dilute solution separation- Batch and continuous reactors for the adsorption and degradation of 1,2-dichlorobenzene from dilute waste water streams using titania as a photocatalyst," *Separation and Purification technology*, **28**, 87-102 (2002).
- Mohseni, M. and A. David, "Gas phase vinyl chloride (VC) oxidation using TiO<sub>2</sub>-based Photocatalysis", *Applied Catalysis B: Environmental*, **46**, 219-228 (2003).
- Montgomery, D.C., "Design and Analysis of Experiments," 3rd ed., Wiley, New York (1991).
- Ollis, D.F. and H. Al-Ekabli, *Photocatalytic Purification and Treatment of Water and Air*, Elsevier, Amsterdam (1993).
- Pengyi, Z., L. Fuyan, Y. Gang, C. Qing and Z. Wanpeng, "A comparative study on decomposition of gaseous toluene by O<sub>3</sub>/UV, TiO<sub>2</sub>/UV and O<sub>3</sub>/TiO<sub>2</sub>/UV," *Journal of Photochemistry and Photobiology A: Chemistry*, **156**, 189-194 (2003).
- Shen, Y.S. and Y. Ku, "Treatment of gas-phase Volatile Organic Compounds (VOCs) by the UV/O<sub>3</sub> process," *Chemosphere*, **38**, 1855-1866 (1999).
- Sirisuk, A., C.G. Hill Jr. and M.A. Anderson, "Photocatalytic degradation of ethylene over thin films of titania supported on glass rings," *Catalysis Today*, **54**, 159-164 (1999).
- Wang, J.H. and M.B. Ray, "Application of ultraviolet photooxidation to remove organic pollutants in the gas phase," *Separation and Purification Technology*, **19**, 11-20 (2000).
- Wang, W., L.W. Chiang and Y. Ku, "Decomposition of benzene in air streams by UV/TiO<sub>2</sub> process," *Journal of Hazardous Materials*, **B101**, 133-146 (2003).
- Zhang, P. and J. Liu, "Photocatalytic degradation of trace hexane in the gas phase with and without ozone addition: kinetic study," *Journal of Photochemistry and Photobiology A: Chemistry*, **167**, 87-94 (2004).

Received: October 2, 2009.

Accepted: December 10, 2009.

Recommended by Subject Editor: Alcântara Pessôa.